Decomposition of cyanobacterial bloom contributes to the formation and distribution of iron-bound phosphorus (Fe-P): Insight for cycling mechanism of internal phosphorus loading

Zhicong Wang [a], Shun Huang [a,b], Dunhai Li [a,*]

[a] Key Laboratory of Algal Biology, Institute of Hydrobiology, Chinese Academy of Sciences, Wuhan 430072, PR China
[b] University of Chinese Academy of Sciences, Beijing 100049, PR China

HIGHLIGHTS

- The higher eutrophication of lake area, the higher Fe-P content in sediments
- Fe-P content in sediments was positively correlated with settled cyanobacteria.
- Simulation experiments confirmed that cyanobacterial biomass promote the Fe-P formation.
- Decomposition of cyanobacterial organic matters contributes to the Fe-P formation.
- We should combine bloom removal and sediment dredging to control lake eutrophication.

GRAPHICAL ABSTRACT
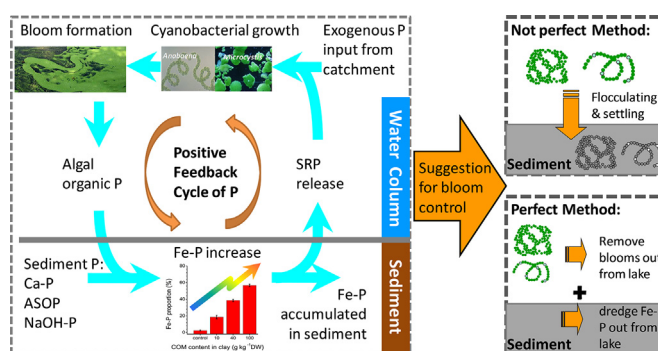
ARTICLE INFO

ABSTRACT

Lake eutrophication and the resulting cyanobacterial blooms have become a global water environment problem. These eutrophic lakes usually have relatively high internal phosphorus loading such as Fe-P to support the formation of cyanobacterial blooms. In order to reveal the mechanisms and processes of phosphorus cycling in lake sediments, in this study, Lake Chaohu was selected as the research area, and the effects of cyanobacterial bloom decomposition on the horizontal distribution pattern of Fe-P was studied by field investigation and laboratory simulations. According to the phosphorus fractions in the sediments, Lake Chaohu can be divided into three lake areas, and the Fe-P content in western Chaohu is the highest (908.6 ± 54.9 mg kg^{-1}). The contents and proportions of Fe-P were significantly positively correlated with cyanobacterial pigments in sediments, but they negatively correlated with undegraded chl-a, especially when the Fe-P content was <400 mg kg^{-1}. Based on these statistical analyses, we proposed a hypothesis that the settled cyanobacterial organic matters (COM) could promote the formation of Fe-P. This hypothesis was proved by the simulation experiments of adding COM to the oligotrophic lakeshore clay. The results suggested that the content and proportion of Fe-P in sediments were significantly increased by the COM addition, and also, they were significantly positively correlated with the decomposition of the COM. The formation processes of Fe-P were further confirmed by the analysis of Fourier transform infrared (FT-IR) spectra. Microbial community analysis suggested that the bacterial species including FeOB and genus *Pseudomonas* might play an important role in the formation of Fe-P. This study suggested that the settled COM could enhance the eutrophication of sediments through a positive feedback cycle. Therefore, it is necessary to carry out bloom removal and sediment dredging simultaneously, and only then the cyanobacterial bloom can be effectively controlled.

© 2018 Elsevier B.V. All rights reserved.

* Corresponding author.
E-mail addresses: wangzc@ihb.ac.cn (Z. Wang), huangshun@ihb.ac.cn (S. Huang), lidh@ihb.ac.cn (D. Li).

1. Introduction

In some eutrophic lakes, cyanobacterial blooms frequently occur in spring and summer (Wang et al., 2012a; Zhu et al., 2016). During the period of blooms, the concentrations of total phosphorus (TP) significantly increased in water column, which was partly attributed to the mass release of labile phosphorus such as Fe-P from sediments (Petticrew and Arocena, 2001; Wang et al., 2016a; Cao et al., 2016). Some researchers suggested that cyanobacterial growth could directly use sedimental phosphorus, and the bloom formation process usually had a "pumping effect" on the Fe-P in sediments (Xie et al., 2003). Others reported that cyanobacterial blooms could induce the release of labile phosphorus such as Fe-P from the sediment into the overlying water (Hao et al., 2016). In some lakes with serious eutrophication, even though external pollution was intercepted completely, the release of sedimental phosphorus was enough to keep the concentration of soluble reactive phosphorus (SRP) in water column at a relatively stable level (Zhou et al., 2001). This low concentration and continuous release of phosphorus would be in favor of the growth of cyanobacteria due to their high affinity for phosphate (Aubriot and Bonilla, 2012).

Sediment is an important storage pool for phosphorus, and it continuously exchanges phosphorus with the overlying water (Petticrew and Arocena, 2001). After the external phosphorus inputs were controlled and reduced, the internal phosphorus loading in sediment is a key factor that influences the restoration of eutrophic water bodies (Ho and Michalak, 2017; Paytan et al., 2017). Generally, release of phosphorus in sediment is recognized as the main pathway of phosphorus supplement for the formation of cyanobacterial blooms (Cao et al., 2016). The release characteristics of sedimental phosphorus were determined by its composition, that is, the higher the content and proportion of Fe-P, the greater the risk of phosphorus release (Chen et al., 2015). Therefore, Fe-P content is considered to be an important indicator of phosphorus release potential of sediments, especially under anaerobic conditions.

Fe-P mainly refers to the phosphorus adsorbed on the surface of iron hydroxide colloid (FeOOH) through physical or chemical actions (Kim et al., 2011), so its release process is affected by many environmental factors such as particle size, pH, especially oxidation-reduction potential (ORP) (Lake et al., 2007; Berbel et al., 2015; Li et al., 2016a. When ORP decreased, Fe^{3+} would be reduced to Fe^{2+}, which further caused the solubility of FeOOH and the release of Fe-P (House and Denison, 2000). Conversely, high ORP would lead to the oxidation of Fe^{2+} to Fe^{3+} and the formation of Fe-P (Peng et al., 2007). Previous study reported that the distribution and formation of Fe-P were closely related to human activities such as the discharge of sewage and industrial waste water (Lu et al., 2010). These researches have compelled lake managers to take actions to reduce the impacts of human activities on eutrophic lakes (Qin et al., 2006; Sadeghi, 2018). However, as so far, these lake protection strategies did not work as expected, and cyanobacterial blooms still occurred frequently despite substantial declines in watershed phosphorus loading (James, 2017), which might be explained by the internal phosphorus cycle between cyanobacterial blooms and sediment (Chen et al., 2014).

At present, many researchers have focused their attention on the mutual effects between Fe-P release and cyanobacterial blooms (Pearce et al., 2013; Wang et al., 2016a; Chen et al., 2018), but few studies have clearly illuminated where the Fe-P come from and what effects of declined blooms on Fe-P formation in sediments. Our previous study suggested that it was a common phenomenon that cyanobacterial blooms declined and settled on the surface of sediment in autumn and winter (Wang et al., 2012a; Wang et al., 2012b; Wang et al., 2012c). These dying cyanobacterial bloom might favor the growth and reproduction of microbes including microaerobic iron (II)-oxidizing bacteria (FeOB) (Emerson et al., 2010). In areas where water re oxygenation frequently occurs, FeOB can oxidize Fe^{2+} into Fe^{3+} and produce the metabolite of FeOOH colloid, which can strongly absorb PO_4^{3-} and promote the formation of Fe-P (Chen et al., 2016). In this study, a typical eutrophic lake, Chaohu, was selected as the study area. We aimed to explore the effects of cyanobacterial bloom decomposition on the distribution of Fe-P, and attempt to reveal the formation mechanisms of Fe-P in sediments. It is hoped that this study can provide a scientific basis for controlling cyanobacterial blooms and internal nutrient loading in eutrophic lakes.

2. Materials and method

2.1. Sampling sites

A total of 37 sampling sites were set in Lake Chaohu, and most of the sites were in the western lake due to its severe eutrophication. The specific distribution of sites was shown in Fig. 1. Surface sediments with 1–5 cm depth were collected by Pedersen sampler and immediately stored at 4 °C. Then, 1.5 g fresh sediment was used to measure the content of various phosphorus forms, and 20 g sediment was freeze-dried and used to analyze the microbial communities by the method of High-throughput sequencing shown in the following title 2.7.

2.2. Extraction and measurement of various pigments in sediment

Organic pigments in sediments can effectively reflect the changes of primary productivity in lakes (Swain, 1985), and it mainly including planktonic and benthic algae (Steinman et al., 1998), phototrophic sulfur bacteria (Hurley and Garrison, 1993), and aquatic plants and higher plants (Bianchi et al., 1993). Among these pigments, myxoxanthophyll (Myx) is one of pigments unique to cyanobacterial species, and it is usually used to indicate the biomass of cyanobacteria in sediments due to hard degradation in anaerobic conditions. The measurement of pigments in sediments was according to the method of Swain (1985) with some modifications. A freeze-dried sample weighing 10.000 g was placed in a 50 mL centrifuge tube and added with 20 mL 90% acetone. The tube was then sealed and sonicated for 5 min with ultrasonic cleaner (KQ5200E, Kunshan ultrasonic instrument co. LTD). After extracting for 24 h at 4 °C in the dark, the extract was centrifuged for 8 min with 5000 rpm and the precipitates were washed with 10 mL 90% acetone for another three times. Combined the supernatants into a 50 mL capacity bottle and adjusted the final volume to 50 mL with 90% acetone. Then, 5 mL, 10 mL, and 35 mL of the extracts were used to analyze the contents of chlorophyll, carotenoid, and Myx, respectively.

The absorbance of the above extract (5 mL) at 665 nm was determined and designated as 665B, and the chlorophyll derivative (CD) was calculated by formula (1), then the extract was added with two drops of diluted HCl and its absorbance at 665 nm was labeled as 665A. The native chlorophyll (NC) was calculated according to the formula (2) reported by Lorenzen (1967) with some modification. Ten milliliters of the extract was added into a 125 mL liquid funnel, and subsequently soapnificated for 2 h with 5 mL methanol potassium hydroxide solution (w/v) and extracted for 0.5 h with 20 mL petroleum ether solvent (30–60 °C). The absorbance of the supernatant was measured at 448 nm and the total carotenoid content was calculated by formula (3). The remaining 35 mL extract was poured into a 100 mL tube, and then 20 mL petroleum ether solvent was added. The lower layer of the extract was dried by a termovap sample concentrator (MD 200, Allsheng, China) to 0.5 mL, resuspended in 5 mL anhydrous ethanol, then absorbance at 412 nm, 504 nm, and 528 nm were measured and Myx was calculated using the formula (4) according to the previous study (Swain, 1985).

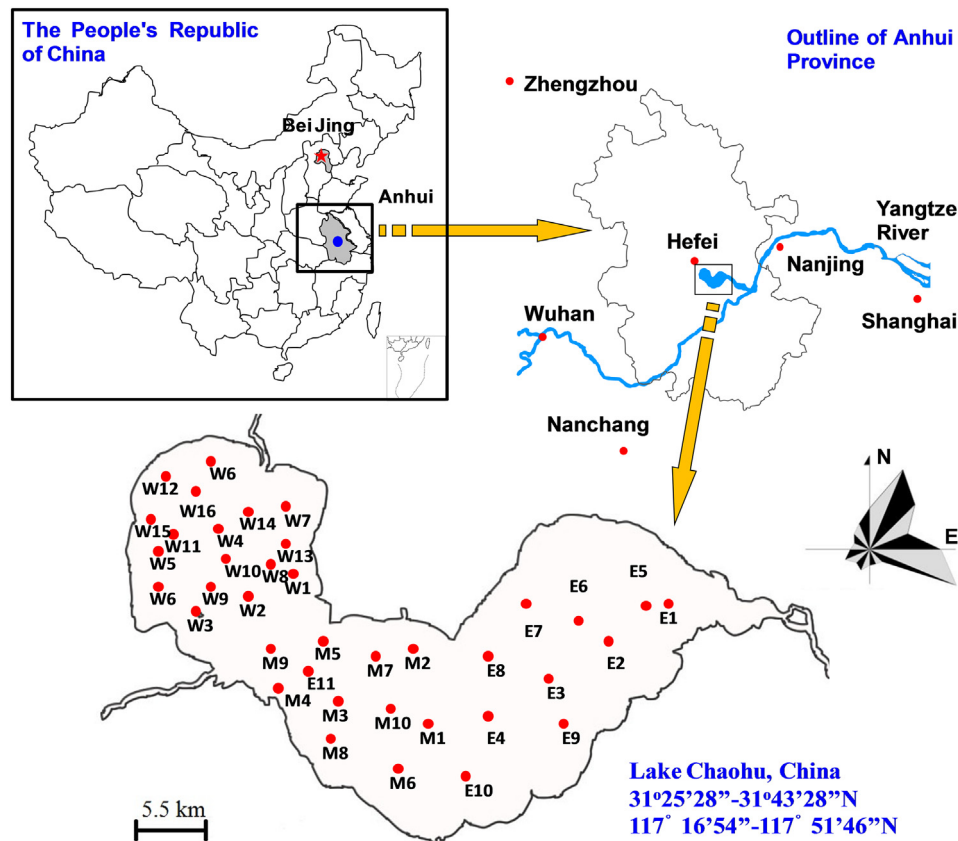$$\text{Chlorophyll derivative (CD)} = \frac{665B \times 50ml}{m_{sample}} \tag{1}$$

Fig. 1. Locations of the sampling sites in Lake Chaohu.

$$\text{Native chlorophyll (NC)} = \frac{665B - 665A}{(0.7 \times 665A)} \times 100\% \qquad (2)$$

$$\text{Total carotenoid (TC)} = \frac{A_{448} \times 100}{m_{sample}} \qquad (3)$$

$$M_{504} = 1.358 \times A_{504} - 1.308 \times A_{528} - 0.031 \times A_{412}; M_{473} = 1.20 \times M_{504}$$
$$\text{Myxoxanthophyll (Myx)} = \frac{10000 \times V \times M_{473}}{2100 \times 0.7 \times m_{sample}}$$
$$\qquad (4)$$

2.3. Measurements of various phosphorus fractions

Sequential extraction of phosphorus from sediment samples was carried out according to the method of Golterman (1996) with some modifications. The 0.5 g sediment samples were accurately placed in centrifuge tubes, and eight phosphorus fractions including water extractable phosphorus (H_2O-P), Fe-P, calcium bound phosphorus (Ca-P), acid soluble organic phosphate (ASOP), glucose bound phosphorus (Sugar-P), nucleic acid and polymeric phosphate (Ploy-P), alkali soluble organic phosphate (NaOH-P), and residual phosphorus (Res-P) were sequentially extracted by adding various extracting reagents as following order: deionized water, 0.05 mol L^{-1} Ca-EDTA and 1% $Na_2S_2O_4$, 0.1 mol L^{-1} Na-EDTA, 0.5 mol L^{-1} H_2SO_4, 0.5 mol L^{-1} TCA (0 °C), 0.5 mol L^{-1} TCA (95 °C), 2 mol L^{-1} NaOH (95 °C), $K_2S_2O_8$ and H_2SO_4. At each step, the sample was oscillated and centrifuged, and the supernatant was taken to measure the various forms of phosphorus, and the residue was retained for the extraction in the next steps. Each sample was measured in parallel twice to minimize experimental errors. In addition, Fe-P, Ca-P, Sugar-P, and Poly-P were extracted for two times so as to ensure the extracting completeness of phosphorus fraction. The advantage of this method is to extract Fe-P and Ca-P firstly, and subsequently use sulfuric acid and sodium hydroxide to extract organic phosphorus. Thus, this method can avoid the mixing of hydrolyzed organic phosphorus into the extraction solution of inorganic phosphorus. The amounts of phosphate in these extracts were determined by the molybdate blue method (Murphy and Riley, 1962). The dry weight of sediment was used to calculate the content of different forms of phosphorus, and all samples were analyzed in triplicate.

2.4. Simulated experiments of Fe-P formation induced by cyanobacterial powder addition

Clay samples collected from the lakeshore zone of Lake Chaohu were used to explore the formation mechanism of Fe-P. Four 500 mL beakers were taken and each was filled with 100 g lakeshore clay, then were respectively added with 0 g, 10 g, 40 g, and 100 g cyanobacterial powder (referred as cyanobacterial organic matter, COM) which dominated by *Microcystis*. Finally, each of these beakers were filled with 300 mL of filtered lake water and cultured at room temperature and low light conditions, and magnetically stirred for 2 h every day. On the 90th day, the experimental clays were collected by centrifugation and then were used to measure various parameters including phosphorus fractionations, Fourier transform infrared (FT-IR) spectroscopy, scanning electron microscopy, pigments content, and high-throughput sequencing of bacterial communities. Each of above experiments was performed three times in parallel.

2.5. Fourier-transform infrared (FT-IR) spectrum

The sediment samples were freeze-dried in a vacuum freeze-drier (ALPHA 1-2, Christ, Germany) and then analyzed using a Fourier-transform infrared (FT-IR) spectrometer according to Xu et al. (2012). Samples were manually ground into fine particles with potassium bromide (KBr) using an agate pestle and mortar. Then, 25 mg (1:40 w/w) of

each powder sample was mixed with 975 mg (39:40 w/w) of KBr. KBr pellets were prepared by exerting a pressure of 10 MPa for approximately 5 min in a pellet press. FT-IR spectra were collected using an Avatar-360 FTIR spectrometer (Thermo Scientific, Waltham, MA) working in the wavelength range of 4000–300 cm^{-1}. For each pellet, 128 scans were performed with a resolution of 4 cm^{-1} at room temperature using OMNIC software.

2.6. Scanning electron microscopy

Clay samples added with COM were collected and air-dried in Petri dishes. Then, the dried clay crusts were cut into small pieces (about 0.3 cm × 0.5 cm) and placed in a vacuum dryer for further drying. These finial dried samples were coated with gold spray and photographed with a scanning electron microscope (Hitachi, S-4800).

2.7. DNA extraction and analysis of microbial community

Approximately 0.50 g of freeze-dried sediment was used to extract DNA using E.Z.N.A™ Mag-Bind Soil DNA Kit (OMEGA Company, USA) according to the manufacture's protocols. Agarose gel was used to detect the integrity of extracted DNA, and the Qubit3.0 DNA test kit was used to quantify the genomic DNA so as to determine the amount of DNA addition in the PCR reaction system. Taking the extracted metagenomic DNA in sediment as template, PCR amplification of 16S rRNA gene (V3, V4 region) was carried out (Fu et al., 2015). 341F primers "CCCTACACGACGCTCTTCCGATCTG (barcode) CCTACGGG NGGCWGCAG" 805R primers "GACTGGAGTTCCTTGGCACCCGAGAATTC CA GACTACHVGGGTATCTAATCC" were used for amplifying the v3 and v4 regions. PCR amplification products were detected by database construction, and the qualified libraries were sequenced by high throughput sequencing on Illumina MiSeq platform.

In order to obtain accurate and high-quality gene sequence information, firstly, Pandaseq (V2.7) software was applied to splice the original sequence and then remove the sequences containing N. Subsequently, Trimmomatic (V0.30) software was conducted to remove the primers and joint sequences, the base with a mass value of <20 at both ends, and the sequences <400 bp in length. Then, the Usearch (V8.0) software was used to compare above sequence with the database, and remove the sequence of chimera sequence, and finally obtained the effective sequence data. Uclust method was used to analyze the cluster information of the operational taxonomic unit (OTU) at an effective data level of 97%. The RDP Bayesian classifier was used to perform taxonomic analysis of the OTU at 97% similar levels, and Silva Library was taken as comparison data (Quast et al., 2013).

2.8. Statistical analysis

Cluster of sampling sites was analyzed by R program (R-3.4.1 for windows) according to phosphorus fractions. All experiments were performed in three replicates and the results were expressed as means and standard deviations. The data were analyzed by using Statistical Product and Service Solutions (version 11.5, SPSS Inc., Chicago, IL, USA). Significant differences were determined by the one-way analysis of variance (ANOVA), and the Duncan's multiple range test was used to perform means comparison. The correlation was analyzed with the Pearson test (two-tailed) at $p = 0.05$. Any differences between the mean values at $p < 0.05$ were considered statistically significant.

3. Results

3.1. Cluster analysis of phosphorus fractions in Lake Chaohu

To reveal the horizontal distribution pattern of various phosphorus especially Fe-P in Lake Chaohu, all of the sampling sites were clustered according to the phosphorus fractions in the sediments. The results suggested that all of the sampling sites can be divided into three categories, which were signed as Cluster I, Cluster II and Cluster III respectively (Fig. 2A). Arranged from high to low, the content order of various phosphorus fractions was Fe-P > Ca-P > NaOH-P > ASOP > Res-P > Poly-P > H$_2$O-P and Sugar-P. Among all phosphorus forms, Fe-P accounted for the largest proportion and it was significantly higher than any other phosphorus fraction.

The difference in phosphorus fractions among the three clusters mentioned above was mainly determined by Fe-P content (Fig. 2B). The Fe-P content of Cluster I located in western Chaohu was as high as 908.6 ± 54.9 mg kg^{-1}, which was significantly higher than those in the middle and eastern regions (i.e. Cluster II and Cluster III, respectively) of Chaohu (523.8 ± 84.8 mg kg^{-1} and 259.6 ± 50.5 mg kg^{-1}, respectively). All of the 37 samples were arranged in order of Fe-P content from high to low, and the first 7 samples were exclusively distributed in the northwest lakeshore area, while most other sampling sites showed a relatively low content of Fe-P. The phosphorus forms of Ca-P, ASOP and NaOH-P were also the main fractions of phosphorus in sediments, but there was no significant difference between their contents in each cluster and that in other clusters.

3.2. Correlations between algal pigments and Fe-P contents

There is a significant correlation between the algal pigment (TC, NC, Myx, and CD) contents and Fe-P contents (Table 1). In general, the contents of algal pigments increased nonlinearly with the increase of Fe-P contents in sediments (Fig. 3). However, there was a significant linear correlation between pigment content and Fe-P content in each cluster mentioned above. The contents of various pigments in Cluster III was significantly higher than those in Cluster I and Cluster II, while there was no significant difference in pigment contents between Cluster I and Cluster II. The distribution boundary of Fe-P content between Cluster III and other two clusters (Cluster I and Cluster II) was very obvious, and its value was about 400 mg kg^{-1} (Fig. 3).

In area of Cluster III where Fe-P contents were lower than 400 mg kg^{-1}, the contents of TC, CD and Myx were significantly positively correlated with the contents of Fe-P. When Fe-P contents were higher than 400 mg kg^{-1}, with the increase of Fe-P, the contents of the three pigments almost remained constant, which were 0.030, 0.288 and 1.455 mg kg^{-1} DW of sediment, respectively (Fig. 3A–C). NC was the percentage of undecomposed chlorophyll in the total chlorophyll, and it had a significant negative correlation with the content of Fe-P. The average value of NC in Cluster I was 20.2%, which was significantly higher than that in Cluster III ($p < 0.01$) (Fig. 3D). These results seemly suggested that the formation of Fe-P might be promoted by the degradation of chlorophyll.

3.3. Proportion changes of Fe-P and Ca-P with pigments

In Cluster III, Myx content in sediments was as low as 0.184 ± 0.046 mg kg^{-1} DW while Fe-P proportion was also very low (0.539 ± 0.013). With the increase of Myx content, the Fe-P proportion significantly linearly increased. In Cluster I and Cluster II, the contents of Myx were respectively 0.291 ± 0.039 mg kg^{-1} DW and 0.285 ± 0.043 mg kg^{-1} DW while the proportions of Fe-P were respectively 0.773 ± 0.056 and 0.698 ± 0.034, which were significantly higher than that in Cluster III ($p < 0.001$) (Fig. 4A). The correlation between chlorophyll contents and Fe-P proportions showed the similar trends as that between Myx and Fe-P (Fig. 4B). These results indicated that the settled cyanobacteria and their decomposition could increase the proportion of Fe-P. However, the linear correlation of Ca-P proportion with the pigment contents was almost opposite to that of Fe-P with pigment contents (Fig. 4C, D). In Cluster I, Ca-P proportion was 0.170 ± 0.009, which was significantly lower than those in Cluster II and Cluster III. There was a significant linear negative correlation between Ca-P proportion and pigment content including chlorophyll and Myx ($p < 0.001$).
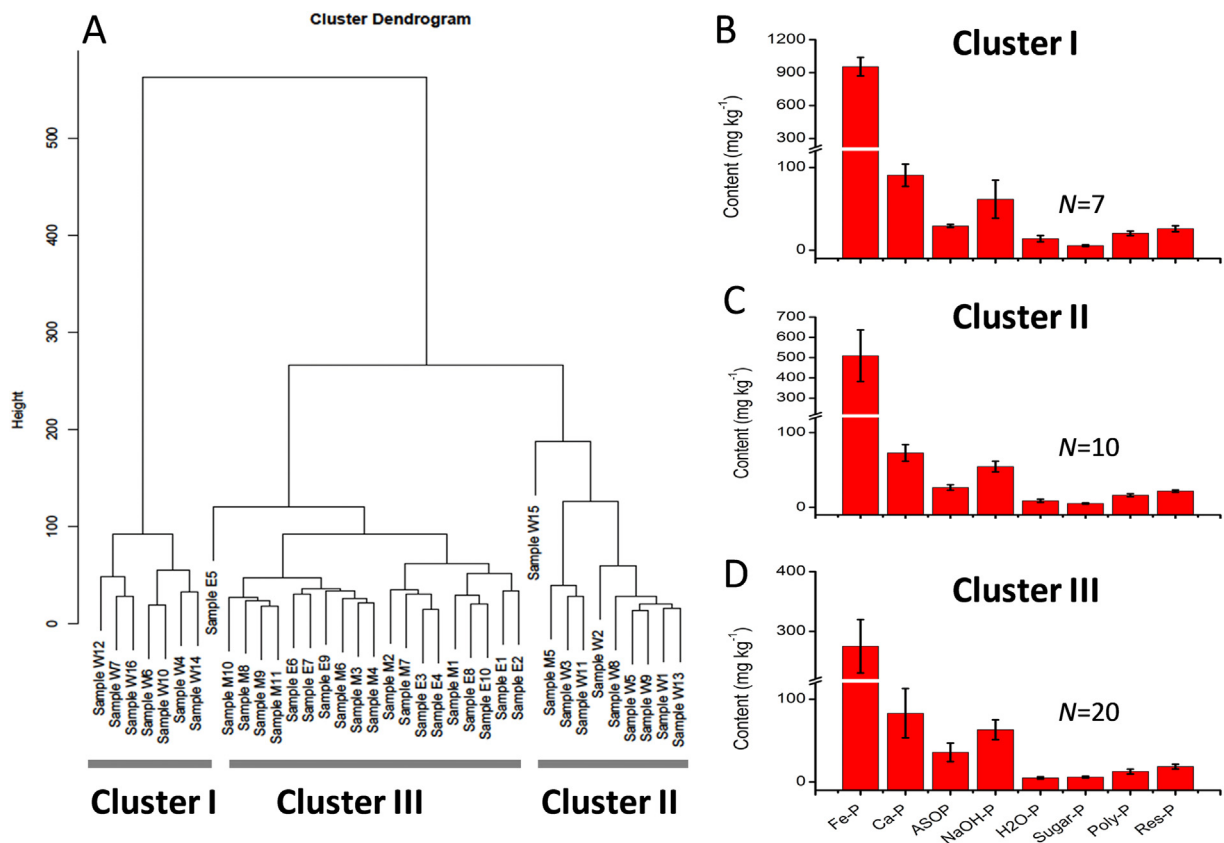
Fig. 2. Cluster analysis of various sampling sites. (A) Cluster analysis of sampling sites according to phosphorus fractions; (B) the average content of phosphorus in each cluster.

3.4. COM addition affected the content and proportion of Fe-P

The total phosphorus (TP) content of lakeshore clay used in the control group was as high as 438.6 mg kg^{-1}, which was calculated by the sum of eight kinds of phosphorus fractions. However, most phosphorus was in inactive forms (Fig. 5A). Res-P was as high as 166.1 mg kg^{-1}, accounting for 37.9% of TP, while Fe-P accounts for only 2.4% of TP (Fig. 5B). After the addition of COM, the contents of Fe-P and Ca-P in the lakeshore clay increased significantly, and ASOP and NaOH-P also increased slightly. When the COM additions were 40 g kg^{-1} DW and

Table 1
Correlation coefficients between pigments and phosphorus fractions in sediment ($n = 37$).

	TC[a]	NC[b]	Myx[c]	CD[d]	H$_2$O-P[e]	Fe-P[f]	Ca-P[g]	ASOP[h]	Sugar-P[i]	Poly-P[j]	NaOH-P[k]	Res-P[l]
TC	1.000											
NC	−0.338[*]	1.000										
Myx	0.733[**]	−0.317	1.000									
CD	0.890[**]	−0.399[*]	0.776[**]	1.000								
H$_2$O-P	0.752[**]	−0.622[**]	0.711[**]	0.761[**]	1.000							
Fe-P	0.742[**]	−0.607[**]	0.699[**]	0.758[**]	0.972[**]	1.000						
Ca-P	0.034	−0.196	0.018	0.025	0.238	0.256	1.000					
ASOP	−0.427[**]	0.145	−0.27	−0.495[**]	−0.274	−0.281	0.658[**]	1.000				
Sugar-P	0.260	−0.204	0.008	0.243	0.344[*]	0.349[*]	0.633[**]	0.244	1.000			
Poly-P	0.656[**]	−0.547[**]	0.598[**]	0.694[**]	0.820[**]	0.840[**]	0.076	−0.475[**]	0.273	1.000		
NaOH-P	0.393[*]	−0.351[*]	0.338[*]	0.540[**]	0.490[**]	0.484[**]	0.323	−0.147	0.423[**]	0.571[**]	1.000	
Res-P	0.095	−0.160	0.216	0.203	0.149	0.06	−0.169	−0.157	0.100	0.089	0.181	1.000

Asterisks indicate p values.
* $p < 0.05$.
** $p < 0.01$.
[a] Total carotenoid per unit dry weight (DW) sediments.
[b] Native chlorophyll per unit dry weight (DW) sediments.
[c] Myxoxanthophyll per unit dry weight (DW) sediments.
[d] Chlorophyll derivative per unit dry weight (DW) sediments.
[e] Water extractable phosphorus per unit dry weight (DW) sediments.
[f] Iron bound phosphorus per unit dry weight (DW) sediments.
[g] Calcium bound phosphorus per unit dry weight (DW) sediments.
[h] Acid soluble organic phosphate per unit dry weight (DW) sediments.
[i] Glucose bound phosphorus per unit dry weight (DW) sediments.
[j] Nucleic acid and polymeric phosphate per unit dry weight (DW) sediments.
[k] Alkali soluble organic phosphate per unit dry weight (DW) sediments.
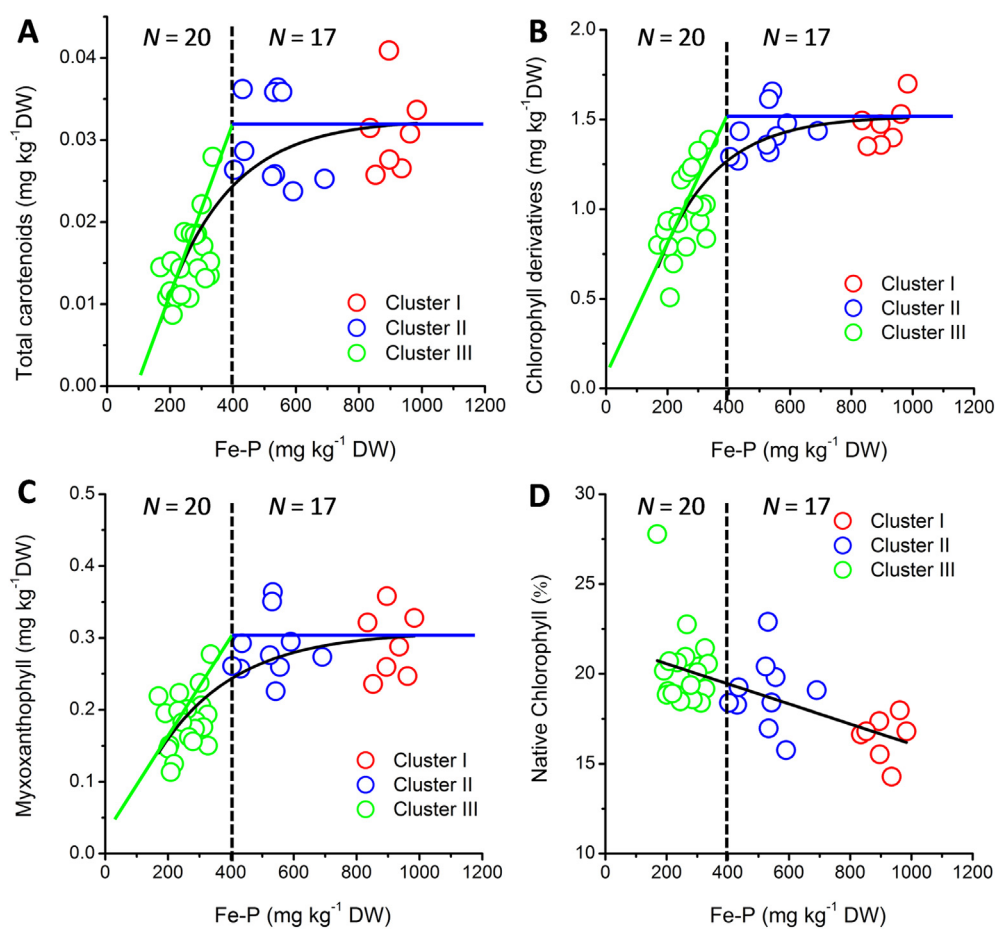[l] Residual phosphorus per unit dry weight (DW) sediments.

Fig. 3. Correlation between Fe-P and various pigments (A) Correlation between Fe-P and total careteniods; (B) Correlation between Fe-P and chlorophyll derivatives; (C) Correlation between Fe-P and myxoxanthophyll; (D) Correlation between Fe-P and native chlorophyll.

100 g kg^{-1} DW of clay, the contents of Fe-P reached 472.4 and 1399.1 g kg^{-1}, respectively (Fig. 5A). The proportion of Fe-P in TP also increased significantly with the addition of COM, and reached 56.9% when the COM addition was 100 mg kg^{-1} (Fig. 5C). With the extension of experimental time, the content and proportion of Fe-P gradually increased (Fig. 5D).

After the addition of COM, Myx content in the lakeshore clay increased significantly, and the content and proportion of Fe-P were significantly positively correlated with Myx content ($p < 0.05$) (Fig. 6A). Meanwhile, the content and proportion of Fe-P showed a significant linear negative correlation with undecomposed chlorophyll ($p < 0.05$) (Fig. 6B).

3.5. Changes of FT-IR spectroscopy

In the infrared absorption spectrum of Fe-P, the absorption peaks at 3400 nm and 1630 nm respectively belong to stretching vibration and deformation vibration of hydroxyl bond (—OH). The peak at 1030 nm belongs to the characteristic absorption peak of Fe-O-P bond, while the absorption range of 995–915 nm corresponds to the P—O bond and 1190–1150 nm corresponds to the P=O bond (Fig. 7A). In comparison with the absorption spectrum of control treatment, the addition of COM could significantly increase these characteristic absorption bands, especially at 3400 nm and 1030 nm (Fig. 7B). This result indicated that the degradation of COM could significantly enhance the formation of Fe-P in the lakeshore clay. We found the absorption peak of Fe-O-P in COM was very low, and it was also very low in the mixture of COM and clay when measured at the initial stage of the experiments. But with the extension of experimental time, the characteristic absorption peaks of Fe-

P in clay mixed with COM gradually increased (Fig. 7C), which suggested that the formation of Fe-P might involve biochemical processes rather than only chemical reactions.

3.6. Characteristics of surface structure

The scanning electron microscopy (SEM) showed that the lakeshore clay without COM addition had obvious shape of mineral particles, and there was no adhesive colloid between these particles (Fig. 8A). After a small amount of COM was added, the surface of the clay particles was covered with a thin layer of colloids (Fig. 8B). A large amount of COM made the clay particles bind together and be totally covered by colloidal organic matters (Fig. 8C, D).

3.7. Composition of microbial community structure

Cluster analysis of microbial community at genus level showed that the lakeshore clay was more similar to the lake sediments rather than clay samples added with COM (Fig. 9). This indicated that the settlement and degradation of COM could significantly alter the structure of microbial community in oligotrophic clays.

Comparing the composition and abundance of microbial communities in clay samples added with different amount of COM, it can be seen that the addition of COM could significantly increase the abundance and proportion of genus *Pseudomonas* (Fig. 10A). However, the abundance of traditional FeOB was very low in all samples, and especially it almost approach to zero in samples with COM addition (Fig. 10B). The typical corresponding environmental factors analysis also showed that the abundance of genus *Pseudomonas* had a relatively
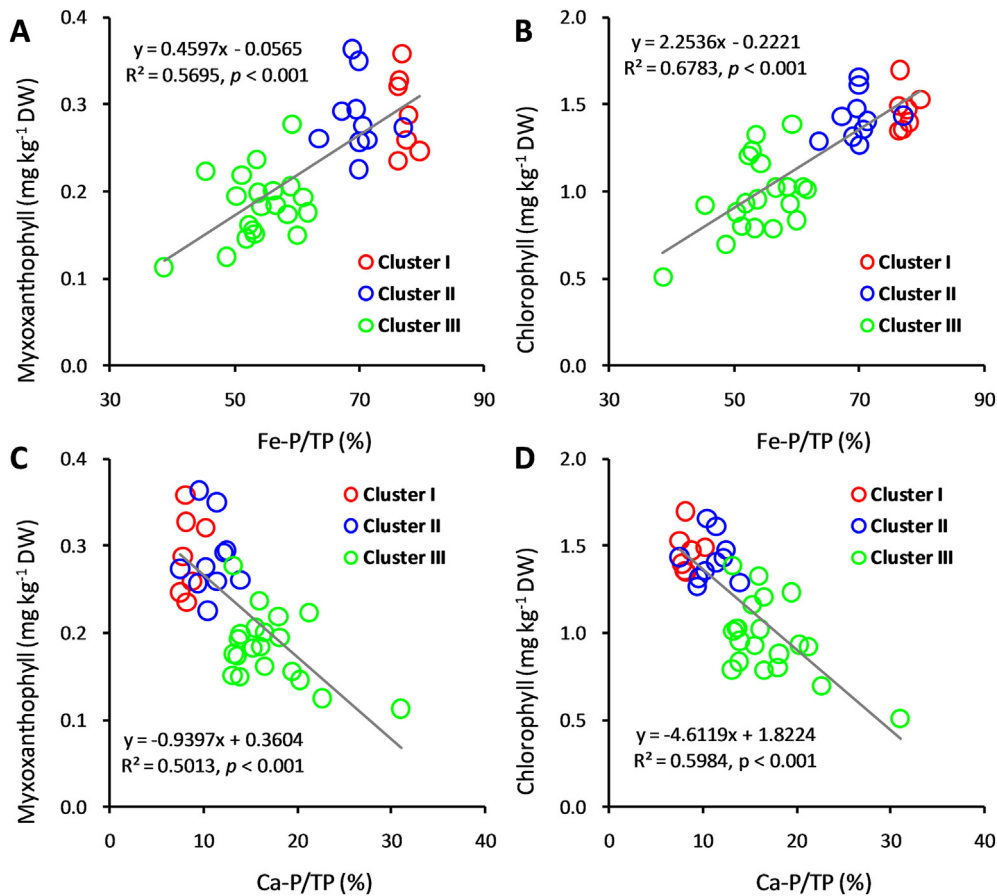
Fig. 4. Correlation between cyanobacterial pigments and the proportions of Fe-P or Ca-P in total phosphorus (TP) (A) Correlation between myxoxanthophyll and Fe-P/TP; (B) Correlation between chlorophyll and Fe-P/TP; (C) Correlation between myxoxanthophyll and Ca-P/TP; (D) Correlation between chlorophyll and Ca-P/TP.

high correlation with the contents of Myx and Fe-P in sediments (Fig. 10C).

4. Discussions

4.1. Distribution pattern of Fe-P in Lake Chaohu

Since Fe-P is a kind of labile phosphorus, and it has a high risk of P-release in eutrophic lakes (Chen et al., 2015), therefore, it is important to explore the correlations between Fe-P content and lake eutrophication. In this study, Lake Chaohu, a large shallow eutrophic lake in the middle and lower reaches of the Yangtze River, was selected as the research area due to the fact that there are different eutrophic states in different lake regions (Wang et al., 2012b). *Anabaena* bloom occurred in late winter and early spring in Lake Chaohu, and it rapidly changed to *Microcystis* bloom in summer and lasted until autumn (Wang et al., 2012c). The distribution of cyanobacterial blooms in Chaohu showed distinct regional characteristics, and the algal biomass in the western lake was usually significantly higher than that in the eastern region (Li et al., 2017). Some researchers reported that the biomass of cyanobacterial bloom was closely related to the release characteristics of phosphorus in sediments (Cao et al., 2016; Liu et al., 2016).

In this study, the results showed that Fe-P accounted for the largest proportion of total phosphorus in sediments, and the distribution of Fe-P also presented a distinct regional pattern. The content of Fe-P in western Chaohu was significantly higher than that in the central and eastern lakes, and its distribution pattern was consistent with that of cyanobacterial blooms (Li et al., 2017). This can be explained by the fact that the Fe-P in sediments is easily released to the water column under anaerobic conditions and promotes the formation of

cyanobacterial blooms (Roden and Edmonds, 1997; Li et al., 2016b). Therefore, the distribution of Fe-P in sediments is closely related to the eutrophication of lakes. This result was inconsistent with previously reports that Fe-P in oligotrophic lakes was higher than that in eutrophicated lakes (Gonsiorczyk et al., 1998), probably because the lakes in previous report were deep stratified lakes (the average depth were 22.8 m and 16.1 m, respectively) while Lake Chaohu in our study is a large shallow lake (only 1.8 m in depth).

Although there was no significant difference in TP content between the sediments in the eastern Chaohu and the clay collected from the lakeshore zone, we found both of the contents and proportions of Fe-P in the former were significantly higher than those in the latter. This indicates that the migration and decomposition processes of cyanobacterial blooms might have a significant effect on the formation and distribution of Fe-P in lake sediments.

4.2. Is settled COM the cause or the result of Fe-P formation?

Microcystis blooms declined in autumn and winter (Wang et al., 2012a), and a large number of algal biomass settled on the surface of sediments (Preston and Stewart, 1980; Reynolds et al., 1981; Brunberg and Peter, 2002; Ma et al., 2016). At relatively low temperatures in autumn or early winter, most of these settled *Microcystis* will lose photosynthetic activity and gradually degrade, and only a few *Microcystis* cells can succeed in overwintering and become the population source of blooms in the coming year (Wang et al., 2016b). In this study, the pigments chlorophyll and Myx were used to represent the settled biomass of photoautotrophic organisms and COM, respectively. The results showed there was a significant positive correlation between chlorophyll and Myx (Supplement 1; Table 1), indicating that the
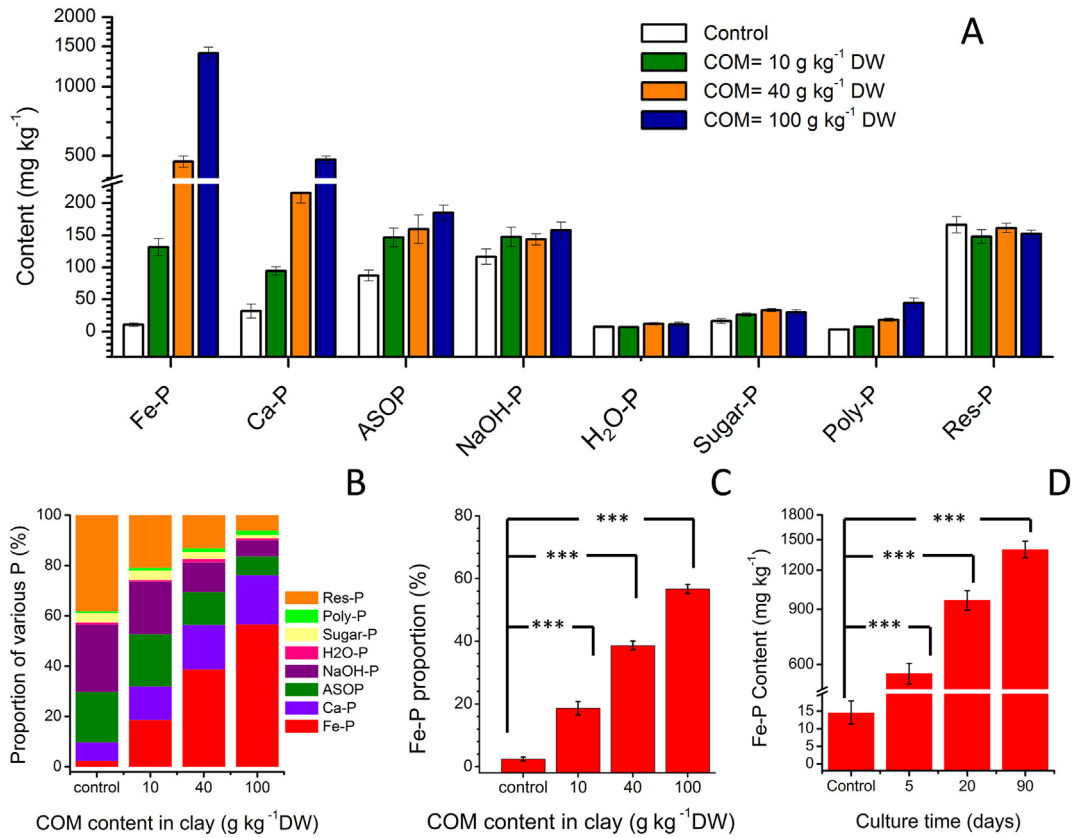
Fig. 5. Effects of COM addition on the phosphorus fractions in the clay collected from lakeshore zone. (A) The effects of COM addition on the contents of various phosphorus fractions; (B) Effects of COM addition on the proportions of various phosphorus fractions; (C) Effects of COM addition on the content of Fe-P; (D) Change of Fe-P content in the clay with the time increasing after the COM addition of 100 g kg^{-1} DW.

pigments in the sediments were mainly contributed by settled COM instead of other algae or higher plants. In the western Chaohu where *Microcystis* blooms frequently occurred, the content of Myx in the sediments was significantly higher than that in other areas, suggesting that *Microcystis* bloom might settle in situ during the decline period. It was known that Fe-P release was an important phosphorus source for the formation of cyanobacterial blooms (Xie et al., 2003; Wang et al., 2016a; Supplement 2A), and it was positively correlated with the settled COM (Fig. 3 and Fig. 4) and with the algal nucleic acid phosphorus (Supplement 2B; Table 1) in this study. Therefore, we can conclude that the settled COM may be the result of Fe-P distribution.

The release of Fe-P in sediments is bound up with the redox conditions of water, and anaerobic conditions will cause the Fe-P to release into overlying water (Li et al., 2016b). The continuous release of Fe-P should inevitably lead to a significant decrease of the Fe-P content and proportion in sediments. However, cluster analyses suggested that Fe-P in the hypertrophic western Chaohu was higher than that in the mesotrophic eastern area. Therefore, we wonder how this Fe-P forms and how it accumulates in eutrophic areas. Some studies have shown that human activities such as wastewater discharge have a certain impact on the distribution of Fe-P in eutrophic water bodies (Ruban et al., 1999; Liu et al., 2017a). But we found that in shallow lakes such as
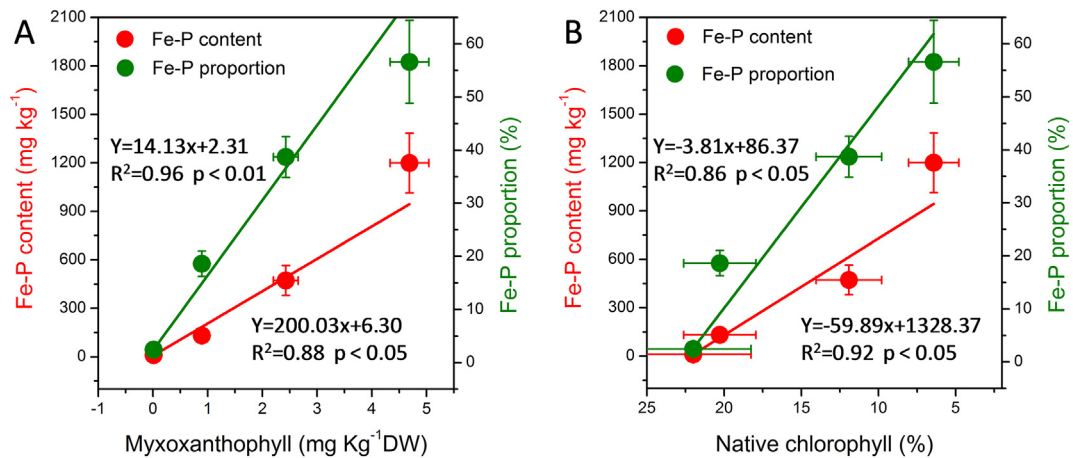

Fig. 6. Correlation between cyanobacterial pigments and Fe-P after the addition of COM. (A) Correlation between myxoxanthophyll and the content or proportions of Fe-P; (B) Correlation between native chlorophyll and the content or proportions of Fe-P.
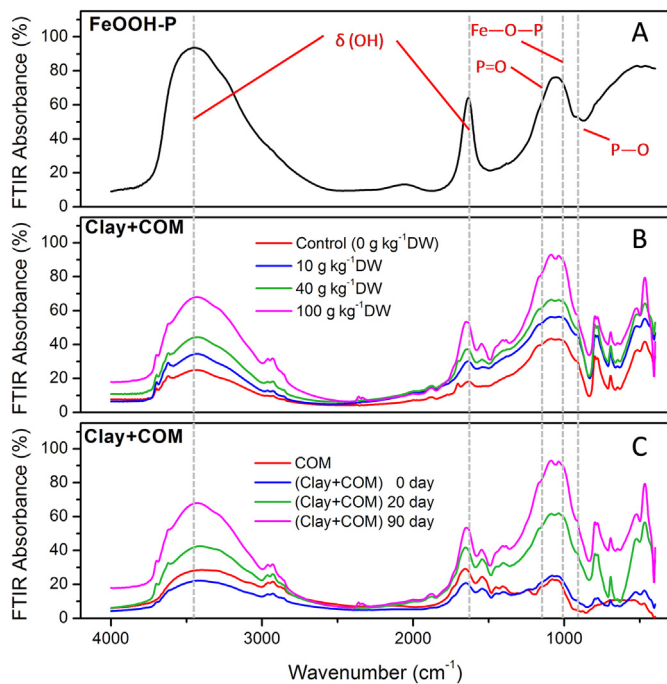
Fig. 7. Changes of Fourier-transform infrared (FT-IR) spectra of FeOOH-P or the clay with COM addition. (A) Characteristic FT-IR absorption spectrum of FeOOH-P; (B) The effects of COM additions on the FT-IR absorption spectra of the clay; (C) Changes of FT-IR absorption spectrum of the clay with the time increasing after the COM addition of 100 g kg^{-1} DW.

Chaohu, there was a significant difference in Fe-P contents between sampling sites that were geographically close and affected by the same human activities, especially in the western Chaohu. This suggests that besides human activities, other factors may play a key role in the distribution of Fe-P. If assume that the migration of Fe-P from sediments to cyanobacterial blooms is an irreversible process, the continuous

release of Fe-P will result in a negative correlation between Fe-P and COM in sediments. However, this study showed that the Fe-P content was significantly positively correlated with the COM amount indicated by the Myx content (Table 1; Figs. 3–6), indicating that the decomposition of COM in sediment had significant effects on the formation of Fe-P. This speculation was consistent with the previous report that the settled cyanobacterial blooms had some effects on the phosphorus cycling in sediments (Chen et al., 2014). Therefore, the settled COM is also the main cause of Fe-P formation in sediment.

4.3. The promoting effects of COM on the formation of Fe-P

There are some studies suggested that the SRP released from sediment is enough to support the rapid growth of cyanobacterial bloom, even though there is no any input from catchment (Xie et al., 2003). Therefore, the release of internal phosphorus loads in lakes is possibly the main reason for the formation of cyanobacterial blooms, especially after the strengthening of lake pollution management by the lake administration in recent years. Based on this analysis, the internal transformation rather than catchment input might play a leading role in the formation and accumulation of Fe-P in sediments.

The lake investigation showed that with the increase of the settled COM, the content as well as the proportion of Fe-P in sediments increased linearly, and the Fe-P content was negatively correlated with the undecomposed cyanobacterial biomass in sediments. These results suggested that (1) the settled COM could affect the content and proportion of Fe-P in sediments; (2) the more the COM in sediments, the higher the degree of its degradation; and (3) the degradation process of COM could promote the formation of Fe-P. The COM in sediment could significantly increase the activity of alkaline phosphatase (APA) (Trojanowska and Izydorczyk, 2010; Wang et al., 2012d) and accelerate the mineralization of organic phosphorus into PO_4^{3-} (Fitzgerald and Nelson, 1966; Harke et al., 2012; Yoko et al., 2014). Under oxidation conditions caused by re oxygenation of water body, Fe^{2+} in sediment could be oxidized into Fe^{3+} and favor for the formation of FeOOH colloid, which could absorb lots of PO_4^{3-} to form Fe-P (Jensen et al.,
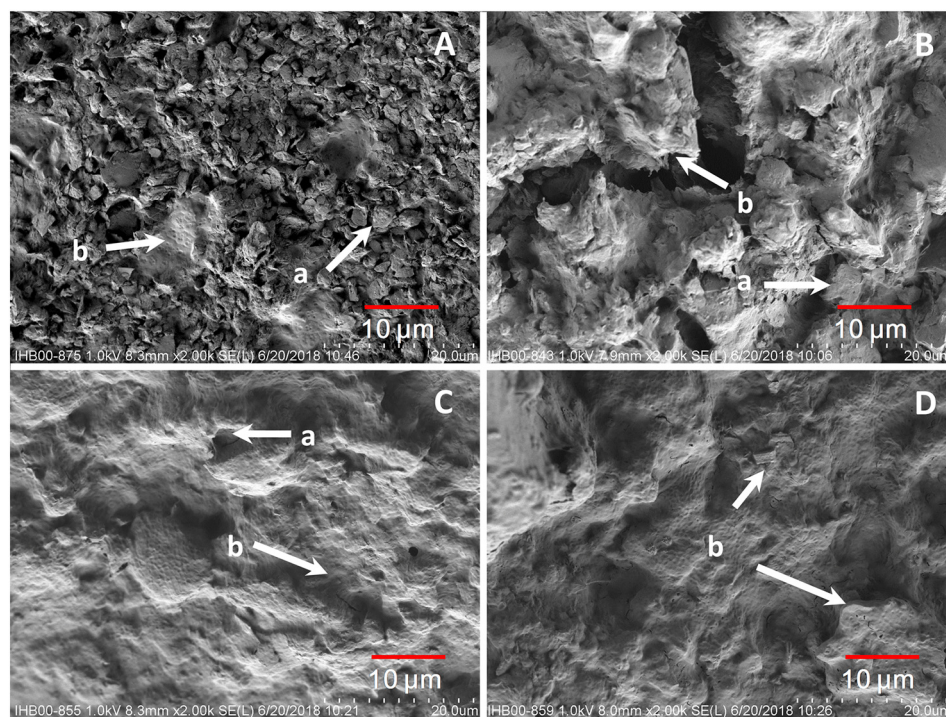

Fig. 8. Ultrastructural characteristics of clay after addition with various dose of COM. (A) No COM addition; (B) COM addition is 10 g kg^{-1} DW; (C) COM addition is 40 g kg^{-1} DW; (D) COM addition is 100 g kg^{-1} DW. In this figure, "a" indicates granular clay particles, and "b" indicates clay particles coated with a layer of colloids.
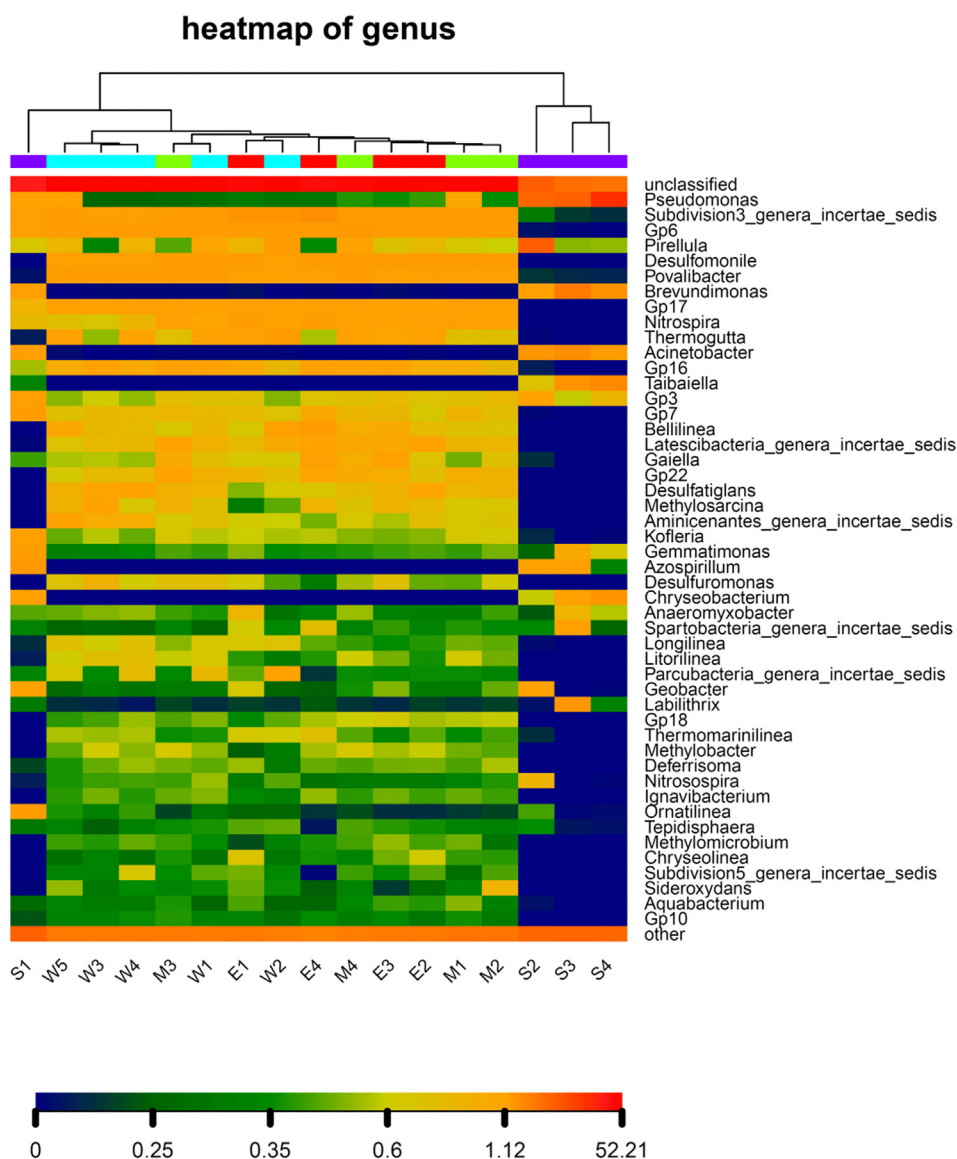
heatmap of genus

Fig. 9. Genus heatmap of microbial community of the samples collected in Lake Chaohu and in simulation experiments.

1995). We found that with the increase of COM in sediments, the proportion of Fe-P increased while the proportion of Ca-P decreased, which suggested that the settled COM could promote the transformation of Ca-P into Fe-P, possessing a greater risk of phosphorus release than that before. This result might be partly explained by the fact that organic phosphate-mineralizing bacteria (OPB) can transform Ca-P into PO_4^{3-} and contribute to the formation of Fe-P.

To further verify the effects of cyanobacterial decomposition on the formation of Fe-P, we added COM into oligotrophic clay collected from the lakeshore zone of Chaohu. On the 90th day of the experiments, we found the Myx content in clay was positively correlated with the amount of COM addition, which further indicated that Myx was a reliable indicator for the settled COM. The initial content and proportion of Fe-P in both of the lakeshore clay and COM were very low, and they significantly increased after the addition of COM (Fig. 5), confirming that the settlement of cyanobacterial bloom can indeed enhance the formation of Fe-P in sediments. Also, the simulation experiments showed that the Fe-P content was significantly correlated to the degradation degree of chlorophyll (Fig. 6), which was consistent with the lake investigation results. This indicated that the decomposed cyanobacterial biomass, rather than the fresh cyanobacterial biomass, led to the formation of Fe-P in sediments. And this speculation was further confirmed by

the results of FT-IR spectroscopy (Fig. 7). However, unlike the results of field investigation, there was no transformation trend of Ca-P to Fe-P in simulation experiments, which may be explained by the inhibition of Ca-P degradation due to the release of excess PO_4^{3-} during the period of bloom degradation.

4.4. The role and mechanism of microorganisms in the formation of Fe-P

In samples of Cluster III, the Fe-P content in sediments was relatively low (Fe-P < 400 mg kg^{-1}), and it was linearly correlated with the settled cyanobacterial biomass. Scanning electron microscopy (SEM) showed that the addition of COM made the surface of clay particles be coated with a layer of organic matters, which may change the physicochemical properties of sediments. Some studies have shown that the degradation of COM can alter the structure of microbial community around algal colonies (Shao et al., 2014). We found that the abundance of iron- metabolizing bacteria in sediments of Cluster I (western Lake Chaohu) was higher than that in Cluster III. Abundant COM and low redox potential of sediments will favor the growth of microaerophilic heterotrophic FeOB and the formation of FeOOH colloid (Emerson et al., 2010). Therefore, we speculate that in the area where there is little COM, the
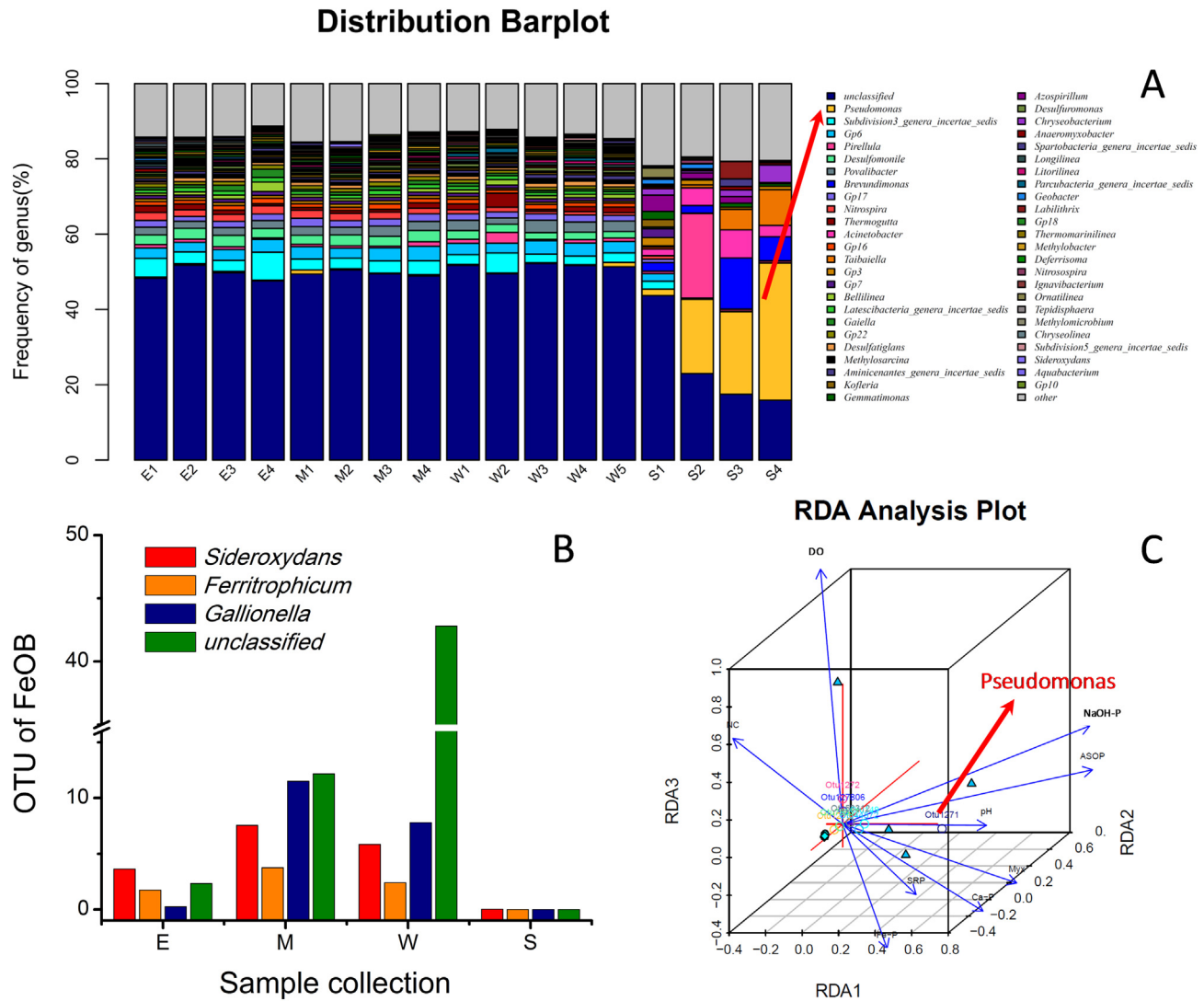
Distribution Barplot

Fig. 10. Composition analysis of microbial community and its correlation with environment factors. (A) Composition analysis of microbial community; (B) OUT abundance of FeOB; (3) The correlation between the microbial community and environment factors.

formation of Fe-P mainly depends on the adsorption of FeOOH colloids to PO_4^{3-} in overlying water.

The COM contents in the sediments of Cluster I and Cluster II were higher than those of Cluster III. The Fe-P contents showed a nonlinear positive correlation with the accumulation of COM in Cluster I and Cluster II, indicating that the rate of Fe-P increasing was higher than that of COM accumulating. Moreover, the proportion of Fe-P linearly increased with the TP in sediments. Therefore, we deduce that plenty of COM would accelerate the mineralization of organic phosphorus, thereby increasing the adsorption rate and capacity of FeOOH colloids for PO_4^{3-}. The analysis of microbial community suggested that the abundance of bacteria in COM treatment groups and Cluster I were significantly higher than those in Cluster III (Supplement 3), and the redox potential of the former was also higher than that of the latter (data not shown). These suggested that excessive COM may promote the growth of anaerobic bacteria such as OPB and enhance the release of PO_4^{3-} from degraded bloom, and subsequently, a large number of PO_4^{3-} were adsorbed by FeOOH colloid and transformed into Fe-P. This speculation can be supported by the promoting effects of COM on the growth of OPB and the activity of APA (Wang and Shen, 2011; Liu et al., 2017b). The analysis of microbial community also suggested that genus *Pseudomonas* played an important role in the formation of Fe-P, which may be explained by

the fact that most OPB were genus *Pseudomonas* (Ramani, 2014). In the simulation experiments, with the addition of COM, the dissolved oxygen in sediments gradually decreased while the PO_4^{3-} concentration gradually increased (Supplement 3), which further evidenced the above assumption.

4.5. Suggestions for controlling eutrophication

The TP content of the lakeshore clay in Lake Chaohu is as high as 438.6 mg kg^{-1} DW, but most of it is inactive phosphorus, while Fe-P and other labile phosphorus are relatively low. These inactive forms of phosphorus in sediments are generally insufficient to support the formation of cyanobacterial blooms. In fact, this view provides a methodology for cyanobacterial bloom control (Lürling and Oosterhout, 2013; Wang et al., 2016c). In some lakes or reservoirs, once the first cyanobacterial bloom occurs, cyanobacterial blooms tend to occur frequently in the next few years. Even after most of the external phosphorus input was controlled, cyanobacterial blooms still occur frequently in eutrophic lakes such as Lake Chaohu (Zhang et al., 2015) and Lake Taihu (Qin et al., 2018) annually. In the present study, our results showed that after the decline of cyanobacterial blooms, COM could significantly change the phosphorus fractions and increase the risk of phosphorus release from sediments, which was beneficial to the formation of
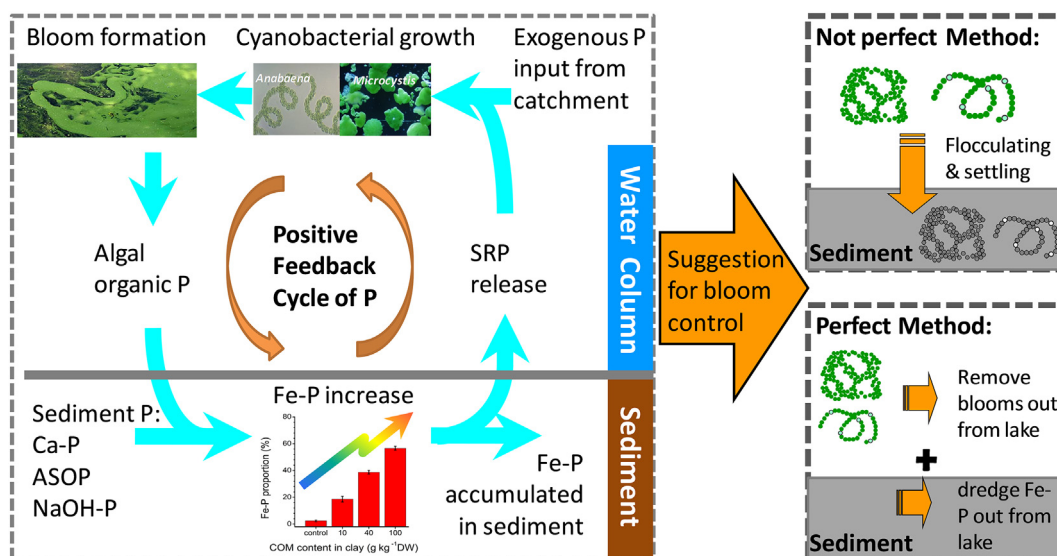
Fig. 11. Schematic diagram of positive-feedback cyclic mechanism of Fe-P and its suggestion for bloom control.

cyanobacterial blooms. The seasonal fluctuation of cyanobacterial blooms in lakes truly reflects the cyclic process between algal organic phosphorus and labile inorganic phosphorus in sediments. This process is a positive feedback cycle as shown in Fig. 11, which can gradually increase internal nutrient loading such as Fe-P to a seriously eutrophic level.

In order to eliminate cyanobacterial blooms, many algal control methods have been proposed, including some methods of flocculating cyanobacterial blooms and settling them onto the surface of sediments (Wang et al., 2012e; Li and Pan, 2013; Ma et al., 2015; Waajen et al., 2018). This study suggested the settled COM could enhance the risk of phosphorus release from sediments, and consequently promote the next cyanobacterial blooms. Therefore, the flocculation method can only transfer the blooms from the water column to the sediment, but it cannot fundamentally control the algal blooms and alleviate the eutrophication of the water body because the nutrients (i.e. nitrogen and phosphorus) are not removed from the eutrophic water. The positive feedback cycling mechanism of phosphorus indicates that there are at least two ways to effectively alleviate the eutrophication of water bodies. One way is to remove algal blooms by mechanical salvage, and another is achieved by dredging sediments. Our present study reveals it is necessary to carry out these two ways simultaneously, only then the SRP will be reduced and the cyanobacterial bloom will be controlled in eutrophic lakes.

5. Conclusions

Based on the phosphorus fractions in the sediments, Lake Chaohu was divided into three lake areas including the western lake, the central lake and the eastern lake by cluster analysis. The Fe-P content in the hypertrophic western area was significantly higher than that in the other two areas. The settled COM in lakes was not only the result, but also the cause of Fe-P distribution. The simulation experiments suggested that COM addition and its degradation could significantly increase the content and proportion of Fe-P in sediments. Microbial community analysis indicated that the bacteria including FeOB and genus *Pseudomonas* might play an important role in the formation of Fe-P. Since there is a positive feedback cycling mechanism of phosphorus between sediments and cyanobacterial blooms, it is necessary to carry out bloom removal and sediment dredging simultaneously, so as to effectively eliminate the cyanobacterial bloom and alleviate the eutrophication of water bodies.

Appendix A. Supplementary data

Supplementary data to this article can be found online at https://doi.org/10.1016/j.scitotenv.2018.10.260.

References

Aubriot, L., Bonilla, S., 2012. Rapid regulation of phosphate uptake in freshwater cyanobacterial blooms. Aquat. Microb. Ecol. 67, 251–263.

Berbel, G.B.B., Favaro, D.I.T., Braga, E.S., 2015. Impact of harbour, industry and sewage on the phosphorus geochemistry of a subtropical estuary in Brazil. Mar. Pollut. Bull. 93, 44–52.

Bianchi, T., Findlay, S., Dawson, R., 1993. Organic matter sources in the water column and sediments of the Hudson River Estuary: the use of plant pigments as tracers. Estuar. Coast. Shelf Sci. 36 (4), 359–376.

Brunberg, A.K., Peter, B., 2002. Benthic overwintering of *Microcystis* colonies under different environmental conditions. J. Plankton Res. 24 (11), 1247–1252.

Cao, X., Wang, Y.Q., He, J., Luo, X.Z., Zheng, Z., 2016. Phosphorus mobility among sediments, water and cyanobacteria enhanced by cyanobacteria blooms in eutrophic Lake Dianchi. Environ. Pollut. 219, 580–587.

Chen, M., Ye, T.R., Krumholz, L.R., Jiang, H.L., 2014. Temperature and cyanobacterial bloom biomass influence phosphorous cycling in eutrophic lake sediments. PLoS One https://doi.org/10.1371/journal.pone.0093130.

Chen, C.Y., Deng, W.M., Xu, X.M., He, J., Wang, S.R., Jiao, L.X., Zhang, Y., 2015. Phosphorus adsorption and release characteristics of surface sediments in Dianchi Lake, China. Environ. Earth Sci. 74 (5), 3689–3700.

Chen, M., Sun, H.Q., Jiang, H.L., 2016. The addition of FeOOH binds phosphate in organic matter-rich sediments. Chem. Ecol. 32 (5), 432–445.

Chen, M.S., Ding, S.M., Chen, X., Sun, Q., Fan, X.F., Lin, J., Ren, M.Y., Yang, L.Y., Zhang, C.S., 2018. Mechanisms driving phosphorus release during algal blooms based on hourly changes in iron and phosphorus concentrations in sediments. Water Res. 133, 153–164.

Emerson, D., Fleming, E.J., McBeth, J.M., 2010. Iron-oxidizing bacteria: an environmental and genomic perspective. Annu. Rev. Microbiol. 2010 (64), 561–583.

Fitzgerald, G.P., Nelson, T.C., 1966. Extractive and enzymatic analyses for limiting or surplus phosphorus in algae. J. Phycol. 2 (1), 32–37.

Fu, S.F., He, S., Shi, X.S., Katukuri, N.R., Dai, M., Guo, R.B., 2015. The chemical properties and microbial community characterization of the thermophilic microaerobic pretreatment process. Bioresour. Technol. 198, 497–502.

Golterman, H.L., 1996. Fractionation of sediment phosphate with chelating compounds: a simplification, and comparison with other methods. Hydrobiologia 335 (1), 87–95.

Gonsiorczyk, T., Casper, P., Koschel, R., 1998. Phosphorus-binding forms in the sediment of an oligotrophic and an eutrophic hardwater lake of the Baltic Lake District (Germany). Water Sci. Technol. 37 (3), 51–58.

Hao, J.C., Lian, B., Liu, H.F., Lu, X.Z., 2016. The release of phosphorus from sediment to lake water induced by cyanobacterial blooms and phosphorus removal by cell harvesting. Geomicrobiol J. 33, 347–353.

Harke, M.J., Berry, D.L., Ammerman, J.W., Gobler, C.J., 2012. Molecular response of the bloom-forming cyanobacterium, Microcystis aeruginosa, to phosphorus limitation. Microb. Ecol. 63 (1), 188–198.

Ho, J.C., Michalak, A.M., 2017. Phytoplankton blooms in Lake Erie impacted by both long-term and springtime phosphorus loading. J. Great Lakes Res. 43 (3), 221–228.

House, W.A., Denison, F.H., 2000. Factors influencing the measurement of equilibrium phosphate concentrations in river sediments. Water Res. 34 (4), 1187–1200.

Hurley, J.P., Garrison, P.J., 1993. Composition and sedimentation of aquatic pigments associated with deep plankton in lakes. Can. J. Fish. Aquat. Sci. 50 (12), 2713–2722.

James, W.F., 2017. Internal phosphorus loading contributions from deposited and resuspended sediment to the Lake of the Woods. Lake Reservoir Manage. 33 (4), 347–359.

Jensen, H.S., Mortensen, P.B., Andersen, F.O., Rasmussen, E.K., Jensen, A., 1995. Phosphorus cycling in a coastal marine sediment, Aarhus Bay, Denmark. Limnol. Oceanogr. 40 (5), 908–917.

Kim, J., Li, W., Philips, B.L., Grey, C.P., 2011. Phosphate adsorption on the iron oxyhydroxides goethite (α-FeOOH), akaganeite (β-FeOOH), and lepidocrocite (γ-FeOOH): a ^{31}P NMR study. Energy Environ. Sci. 4, 4298–4305.

Lake, B.A., Coolidge, K.M., Norton, S.A., Amirbahman, A., 2007. Factors contributing to the internal loading of phosphorus from anoxic sediments in six Maine, USA, lakes. Sci. Total Environ. 373 (2–3), 534–541.

Li, L., Pan, G., 2013. A universal method for flocculating harmful algal blooms in marine and fresh waters using modified sand. Environ. Sci. Technol. 47 (9), 4555–4562.

Li, Z.R., Sheng, Y.Q., Yang, J., Burton, E., 2016a. Phosphorus release from coastal sediments: impacts of the oxidation-reduction potential and sulfide. Mar. Pollut. Bull. 113 (1–2), 176–181.

Li, H., Song, C.L., Cao, X.Y., Zhou, Y.Y., 2016b. The phosphorus release pathways and their mechanisms driven by organic carbon and nitrogen in sediments of eutrophic shallow lakes. Sci. Total Environ. 572, 280–288.

Li, Y.X., Liu, B.B., Liu, S.X., 2017. The trophic state of lake water regulates spatial-temporal variations of bloom-forming Microcystis. Chin. J. Oceanol. Limnol. 35 (2), 415–422.

Liu, J.Z., Luo, X.X., Zhang, N.M., Wu, Y.H., 2016. Phosphorus released from sediment of Dianchi Lake and its effect on growth of Microcystis aeruginosa. Environ. Sci. Pollut. Res. 23 (16), 16321–16328.

Liu, Y., Cheng, Z.Q., Branco, B.F., Marra, J.F., 2017a. Speciation and mobility of phosphate in the eutrophic ponds at Prospect Park, Brooklyn, New York, USA. J. Geosci. Environ. Protect. 5, 26–36.

Liu, Y.Q., Cao, X.Y., Li, H., Zhou, Z.J., Wang, S.Y., Wang, Z.C., Song, C.L., Zhou, Y.Y., 2017b. Distribution of phosphorus-solubilizing bacteria in relation to fractionation and sorption behaviors of phosphorus in sediment of the three gorges reservoir. Environ. Sci. Pollut. Res. 24, 17679–17687.

Lorenzen, C.J., 1967. Determination of chlorophyll and pheopigments: spectrophotometric equations. Limnol. Oceanogr. 12 (2), 343–346.

Lu, S.Y., Jin, X.C., Wu, F.C., Guo, J.N., Si, J., 2010. Spatial distribution of phosphorus forms in sediments with different distances to the estuary of the Dianchi Lake, China. Front. Environ. Sci. Eng. China 4 (3), 295–300.

Lürling, M., Oosterhout, F.V., 2013. Controlling eutrophication by combined bloom precipitation and sediment phosphorus inactivation. Water Res. 47, 6527–6537.

Ma, X.X., Wang, Y.A., Feng, S.Q., Wang, S.B., 2015. Comparison of four flocculants for removing algae in Dianchi Lake. Environ. Earth Sci. 74 (5), 3795–3804.

Ma, J.R., Qin, B.Q., Paerl, H.W., Brookes, J.D., Hall, N.S., Shi, K., Zhou, Y.Q., Guo, J.S., Li, Z., Xu, H., Wu, T.F., Long, S.X., 2016. The persistence of cyanobacterial (Microcystis spp.) blooms throughout winter in Lake Taihu, China. Limnol. Oceanogr. 61 (2), 711–722.

Murphy, J., Riley, J.P., 1962. A modified single solution method for determination of phosphate in natural waters. Anal. Chim. Acta 26 (1), 31–36.

Paytan, A., Roberts, K., Watson, S., Peek, S., Chuang, P.C., Defforey, D., Kendall, C., 2017. Internal loading of phosphate in Lake Erie central basin. Sci. Total Environ. 579, 1356–1365.

Pearce, A.R., Rizzo, D.M., Watzin, M.C., Druschel, G.K., 2013. Unraveling associations between cyanobacteria blooms and in-lake environmental conditions in Missisquoi bay, lake Champlain, USA, using a modified self-organizing map. Environ. Sci. Technol. 47 (24), 14267–14274.

Peng, J.F., Wang, B.Z., Song, Y.H., Yuan, P., Liu, Z.H., 2007. Adsorption and release of phosphorus in the surface sediment of a wastewater stabilization pond. Ecol. Eng. 31 (2), 92–97.

Petticrew, E.L., Arocena, J.M., 2001. Evaluation of iron-phosphate as a source of internal lake phosphorus loadings. Sci. Total Environ. 266, 87–93.

Preston, T., Stewart, W.D.P., 1980. Bloom-forming cyanobacterium Microcystis aeruginosa overwinters on sediment surface. Nature 288 (5789), 365–367.

Qin, B.Q., Yang, L.Y., Chen, F.Z., Zhu, G.W., Zhang, L., Chen, Y.Y., 2006. Mechanism and control of lake eutrophication. Chin. Sci. Bull. 51 (19), 2401–2412.

Qin, B.Q., Yang, G.J., Ma, J.R., Wu, T.F., Li, W., Liu, L.Z., Deng, J.M., Zhou, J., 2018. Spatiotemporal changes of cyanobacterial bloom in large shallow eutrophic Lake Taihu, China. Front. Microbiol. 9. https://doi.org/10.3389/fmicb.2018.00451.

Quast, C., Pruesse, E., Yilmaz, P., Gerken, J., Schweer, T., Yarza, P., Peplies, J., Glöckner, F.O., 2013. The SILVA ribosomal RNA gene database project: improved data processing and web-based tools. Nucleic Acids Res. 41 (D1), D590–D596.

Ramani, V., 2014. Organic phosphate mineralization by Bacillus sphaericus and Pseudomonas cepacia. Int. J. Agric. Technol. 10 (4), 915–922.

Reynolds, C.S., Jaworsky, G.H.M., Cmiech, H.A., Leedale, G.F., 1981. On the annual cycle of the blue-green algae Microcystis aeruginosa Kütz. emend. Elenkin. Philos. Trans. R. Soc. London Ser. B 293, 419–477.

Roden, E.E., Edmonds, J.W., 1997. Phosphate Mobilization in Iron-rich Anaerobic Sediments: Microbial Fe(III) Oxide Reduction Versus Iron-sulfide Formation Archiv fur Hydrobiologie. 139(3) pp. 347–378.

Ruban, V., Brigault, S., Demare, D., Philippe, A.M., 1999. An investigation of the origin and mobility of phosphorus in freshwater sediments from Bort-Les-Orgues Reservoir, France. J. Environ. Monit. 1 (4), 403–407.

Sadeghi, S., 2018. Laboratory evaluation of internal and external nutrient removal to control algal bloom in eutrophic lakes. Electron. Theses Diss. 2476. https://openprairie.sdstate.edu/etd/2476.

Shao, K.Q., Zhang, L., Wang, Y.P., Yao, X., Tang, X.M., Qin, B.Q., Gao, G., 2014. The responses of the taxa composition of particle-attached bacterial community to the decomposition of Microcystis blooms. Sci. Total Environ. 488–489, 236–242.

Steinman, A.D., Havens, K.E., Louda, J.W., Winfree, N.M., Baker, E.W., 1998. Characterization of the photoautotrophic algal and bacterial communities in a large, shallow, subtropical lake using HPLC-PDA based pigment analysis. Can. J. Fish. Aquat. Sci. 55 (1), 206–219.

Swain, E.B., 1985. Measurement and interpretation of sediment pigment. Freshw. Biol. 15, 53–75.

Trojanowska, A.A., Izydorczyk, K.K., 2010. Phosphorus fractions transformation in sediments before and after cyanobacterial bloom: implications for reduction of eutrophication symptoms in dam reservoir. Water Air Soil Pollut. 211, 287–298.

Waajen, G., van Oosterhout, F., Douglas, G., Lurling, M., 2018. Management of eutrophication in Lake De Kuil (The Netherlands) using combined flocculant - lanthanum modified bentonite treatment. Water Res. 97, 83–95.

Wang, Y., Shen, Z.Y., 2011. Release of phosphorus in sediments from a tributary of the three gorges reservoir (China) with phosphate-solubilising bacteria. Int. J. Environ. Pollut. 45, 145–156.

Wang, Z.C., Li, G.W., Li, G.B., Li, D.H., 2012a. The decline process and major pathways of Microcystis bloom in Lake Taihu, China. Chin. J. Oceanol. Limnol. 30 (1), 37–46.

Wang, Z.C., Li, D.H., Li, Z.J., 2012b. Effect of rainfall on the decline of Microcystis (Cyanophyceae) blooms in Lake Chaohu, China. Fresenius Environ. Bull. 21 (8), 2145–2152.

Wang, Z.C., Li, Z.J., Li, D.H., 2012c. A niche model to predict Microcystis bloom decline in Chaohu Lake, China. Chin. J. Oceanol. Limnol. 30 (4), 587–594.

Wang, S.R., Jiao, L.X., Yang, S.W., Jin, X.C., Yi, W.L., 2012d. Effects of organic matter and submerged macrophytes on variations of alkaline phosphatase activity and phosphorus fractions in lake sediment. J. Environ. Manag. 113, 355–360.

Wang, Z.C., Li, D.H., Qin, H.J., Li, Y.X., 2012e. An integrated method for removal of harmful cyanobacterial blooms in eutrophic lakes. Environ. Pollut. 160, 34–41.

Wang, J.Z., Jiang, X., Zheng, B.H., Chen, C.X., Kang, X.M., Zhang, C.Y., Song, Z.Q., Wang, K., Wang, W.W., Wang, S.H., 2016a. Effect of algal bloom on phosphorus exchange at the sediment-water interface in Meiliang Bay of Taihu Lake, China. Environ. Earth Sci. 75 (57), 1–9.

Wang, C.B., Feng, B., Tiang, C.C., Tian, Y.Y., Chen, D., Wu, X.Q., Li, G.B., Xiao, B.D., 2016b. Quantitative study on the survivability of Microcystis colonies in lake sediments. J. Appl. Phycol. 30 (1), 495–506.

Wang, L.J., Pang, G., Shi, W.Q., Wang, Z.B., Zhang, H.G., 2016c. Manipulating nutrient limitation using modified local soils: a case study at Lake Taihu (China). Water Res. 101, 25–35.

Xie, L.Q., Xie, P., Tang, H.J., 2003. Enhancement of dissolved phosphorus release from sediment to lake water by Microcystis blooms—an enclosure experiment in a hyper-eutrophic, subtropical Chinese lake. Environ. Pollut. 122, 391–399.

Xu, L., Cai, C.B., Cui, H.F., Ye, Z.H., Yu, X.P., 2012. Rapid discrimination of pork in Halal and non-Halal Chinese ham sausages by Fourier transform infrared (FTIR) spectroscopy and chemometrics. Meat Sci. 92 (4), 506–510.

Yoko, O., Inoue, T., Yokota, K., Ngoc, N.M., 2014. Availability of different phosphorus forms in agricultural soil to Microcystis aeruginosa. Water Sci. Technol. 69 (6), 1205–1211.

Zhang, Y.C., Ma, R.H., Zhang, M., Duan, H.T., Loiselle, S., Xu, J.D., 2015. Fourteen-year record (2000—2013) of the spatial and temporal dynamics of floating algae blooms in Lake Chaohu, observed from time series of MODIS images. Remote Sens. 7, 10523–10542.

Zhou, Q.X., Gibson, C.E., Zhu, Y.M., 2001. Evaluation of phosphorus bioavailability in sediments of three contrasting lakes in China and UK. Chemosphere 42 (2), 221–225.

Zhu, W., Zhou, X.H., Chen, H.M., Gao, L., Xiao, M., Li, M., 2016. High nutrient concentration and temperature alleviated formation of large colonies of Microcystis: evidence from field investigations and laboratory experiments. Water Res. 101, 167–175.